Tau Protein Preferentially Associates With Synaptic Mitochondria in a Mouse Model of Tauopathy

Andrew J Trease
University of Nebraska Medical Center
Joseph George
University of Nebraska Medical Center
Katy Emanuel
University of Nebraska Medical Center
Howard S Fox
University of Nebraska Medical Center
Kelly Stauch (kelly.stauch@unmc.edu)
University of Nebraska Medical Center https://orcid.org/0000-0001-7444-4403

Research article

Keywords: Aging, Bioenergetics, Proteomics, Synaptic mitochondria, Tau, Phosphorylation

Posted Date: February 11th, 2021

DOI: https://doi.org/10.21203/rs.3.rs-183974/v1

Abstract

Background

A consequence of an aging society is a continual and dramatic increase in the number of patients suffering from tauopathies, including Alzheimer's disease (AD) and certain frontotemporal dementias. Accumulation of intracellular inclusions of abnormal fibrillar forms and hyperphosphorylated forms of microtubule-associated protein tau are hallmarks of AD and other tauopathies. Although tau pathology is associated with neuronal dysfunction the mechanism responsible remains obscure. *In vitro*, pathologically elevated expression of tau alters mitochondrial distribution by impairing cellular trafficking and thus may represent an important mediator of mitochondrial abnormalities contributing to neuronal dysfunction. We used the transgenic htau mouse model of tauopathy to investigate *in vivo* alterations in brain mitochondria in the presence of pathological forms of human tau.

Methods

In this study, we investigated alterations in bioenergetics and profiled the proteome of brain mitochondria from wild-type (WT) and htau mice at ages prior to and coinciding with pathologic tau deposition in htau mice. In addition, we characterized the expression of total and hyperphosphorylated forms of tau associated with synaptic mitochondria by biochemical fractionation and immunoblotting.

Results

Significant tau pathology-dependent alterations in synaptic mitochondrial bioenergetics were observed at 8 mo nths, but not 5 months, of agein htau mice; however, non-synaptic mitochondrial function remained unaltered. Further, compared to control mice, proteins involved in microtubule-based movement were differentially expressed in htau mice at 8 months of age. In addition, significant accumulation of tau and its hyperphosphorylated forms was observed in synaptic mitochondria isolated from 8-month-old htau mice.

Conclusion

These data suggest that tau preferentially associates with synaptic mitochondria as compared to non-synaptic mitochondria, and accumulation of pathologic forms of tau coincides with synaptic mitochondrial bioenergetic changes reminiscent of an aged synaptic mitochondrial phenotype reported in aging WT mice. Furthermore, the mitochondrially associated tau is soluble in carbonate buffer and more accessible to protease action suggesting it is not integrated into mitochochondrial membranes, but may rather be the result of protein-protein interactions.

Background

The major histopathological and physiological hallmarks of Alzheimer's disease (AD) are neurofibrillary tangles (NFT), amyloid plaques, neuronal loss, and synaptic failure [1]. Synaptic deficits occur very early

in AD and synapse loss is the most predictive of cognitive status [2]. Although soluble oligomeric forms of amyloid-β are implicated in synapse loss early during AD progression, amyloid burden does not correlate well with synapse and neuron loss or severity of AD [2–8]. In contrast, intracellular NFTs, comprised primarily of aberrantly phosphorylated and misfolded microtubule-associated protein tau (Mapt), lead to synaptic alterations and correlate with neuronal loss and cognitive deficits in AD patients more readily than does amyloid burden [2, 6, 9, 10]. Furthermore, while pathogenic deposition of both tau and amyloid affect neuronal health and function, studies have suggested amyloid toxicity is dependent on tau [11–14]. The mechanism by which tau over-expression alters synaptic function remains poorly understood; however, mutant and hyperphosphorylated forms of tau have been shown to alter mitochondrial trafficking within neurons *in vitro*, implicating a mitochondrial role in the observed synapse deficits [11, 15–17]. Despite these findings, data from *in vivo* experimental systems is lacking.

Classical investigations into the molecular basis of AD and other dementia related neurodegenerative diseases has primarily focused on the contributions of amyloid (reviewed in [18]). More recently however, scientific and clinical interest in tau protein has begun to grow. Under normal physiological conditions tau proteins interacts with microtubules (MTs) via MT-binding regions, promoting MT stability and fast axonal transport of molecular cargos in neurons [15, 16, 19–25] and are tightly regulated, most notably by post-translational modifications of tau (i.e. phosphorylation) [10, 15, 20, 26–28]. MT-dependent transport of mitochondria into the axon is a critical factor to maintain local adenosine triphosphate (ATP) production in distal neuronal compartments, like the synapse [29, 30]. Despite the importance of tau to normal cellular trafficking, tau knock-out (KO) mice are both viable and lack overt pathology, perhaps due to compensation by other microtubule associated proteins (e.g. Map1A and Map1B) [31, 32]. This is supported by a study that found tau and Map1B double KO mice suffer a lethal phenotype, dying by 4 weeks of age [33]. Interestingly, primary neuronal cultures from tau KO mice display shortened axonal tracts, decreased microtubular density, and a reduction in the number of cross-bridging between adjacent microtubules as well as between microtubules and the cell membrane [33–35]. Notably, in *in vitro* systems, tau accumulation can drive aberrant mitochondrial accumulation at the synapse [36]; and increased accumulation of tau protein in presynaptic regions has been observed to impair synaptic function [37]. In diseases such as AD, tau is hyperphosphorylated, accumulates in neurons, and forms paired helical filaments (PHFs). As a result, tau loses its ability to bind with microtubules, which ultimately leads to neurodegeneration [26, 27, 38]. Evidence suggests that overexpressed and phosphorylated tau appears to impair axonal transport of organelles causing synapse starvation, depletion of ATP, and neuronal damage [39–41]. In htau mice, tau redistribution from the axons into the cell bodies occurs by 3 months of age, accumulation of hyperphosphorylated tau begins by 6 months of age and increases further by 13 and 15 months of age, aggregated tau and PHFs are detectable by 9 months of age, additionally synaptic dysfunction has been demostrated by electrophysiology [38, 42]. Similarly, to human AD patients the majority of tau pathology in htau mice is found in the neocortex and hippocampus [38, 42].

In the present study we investigated the outcomes of expression of human non-mutant tau and age-dependent tau pathological changes to non-synaptic and synaptic brain mitochondria using

bioenergetics assays, proteomic analysis, and biochemical fractionation experiments in htau mice. These mice express human non-mutant tau (all six isoforms) in the absence of murine tau and suffer progressive tau aggregation and cognitive deficits in conjunction with accumulation of NFTs [38, 42]. Here, in htau mice, elevated levels of tau protein were observed to preferentially associate with synaptic mitochondria compared to non-synaptic. Furthermore, there was a significant increase in synaptic mitochondrial associated tau protein at 8-months of age compared to 5-month old animals in htau mice only. This correlated with both age-dependent levels of tau phosphorylation and alterations in the bioenergetics of synaptic mitochondria. Additionally, carbonate extraction and protease digestion revealed mitochondrially associated tau is associated with, but not inserted into the mitrochondrial surface. We have identified the presence of multiple pathologic forms of tau associated with synaptic mitochondria, indicating a potentially direct role for tau in the impairment of synaptic homeostasis.

Materials And Methods

Experimental design

The aim of this study was to assess the molecular and functional characteristics of brain mitochondria of a mouse model of AD that carries the human tau gene. Brain mitochondria were assessed by bioenergetic assays, quantitative proteomics, and biochemical assessment. A total of 24 samples types were used (2 mouse genotypes * 2 mitochondrial populations * 2 age-points * 3 biological replicates).

Reagents and materials

Animals

Htau mice (B6.Cg-*Mapt*$^{tm1(EGFP)Klt}$Tg(MAPT)8cPdav/J, Stock# 005491; Jackson Laboratory (JAX), (Bar Harbor, ME) express all six isoforms (including both 3R and 4R forms) of human tau in the absence of murine tau. The generation and characterization of the htau mice has been described previously [38]. All mice used in this study were male and aged to 5 or 8 months and for each experimental protocol, transgenic mice were compared to age-matched controls (C57BL/6J mice, Stock# 000664; JAX). Animals were fed standard mouse chow and water ad libitum and housed in a controlled environment under a 12-hour light/dark schedule. Experiments were performed in accordance with National Institutes of Health guidelines under a protocol approved by the University of Nebraska Medical Center Institutional Animal Care and Use Committee.

Reagents

All chemicals and reagents were purchased from Sigma Aldrich (St. Louis, MO) unless noted below.

Antibodies

We used the following antibodies in this study: Tau46 (used in Figs. 4 and 6B; 1:1000, #4019, Cell Signaling Technology, Danvers, MA); Tau (used in Fig. 6C, 1:1000, #46687, Cell Signalling Technology,

Danvers, MA); CP13 Tau, PHF1 Tau, and MC1 Tau (all phospho-tau antibodies were used at 1:25 and obtained from Dr. Peter Davies, Feinstein Institutes for Medical Research); HSP60 (1:1000, #12165, Cell Signaling Technology, Danvers, MA); Total OxPhos Rodent Antibody Cocktail (1:2,000, ab110413, Abcam, Cambridge, MA); VDAC1 (1:2,000, #4661, Cell Signaling Technology, Danvers, MA); SDHA (1:2000, #11998, Cell Signaling Technology, Danvers, MA); goat anti-mouse 680RD (P/N: 926-68070), goat anti-mouse 800CW (P/N: 926-32210), donkey anti-rabbit 680RD (P/N: 926-68073) and goat anti-rabbit 800CW (P/N: 926-32211) (1:20,000, Licor, Lincoln, NE).

Isolation of brain mitochondria

The mice were sacrificed by cervical dislocation and the brain was immediately removed, then rinsed with cold mitochondrial isolation buffer (MSHE): 70 mM sucrose, 210 mM mannitol, 5 mM HEPES, 1 mM EGTA and 0.5% (w/v) fatty acid free BSA (pH 7.2). The protocol was carried out on ice and all subsequent spins were done at 4°C. The brain was homogenized for 10 strokes with a Dounce homogenizer in MSHE containing cOmplete Mini, EDTA-free protease inhibitor cocktail (Roche Diagnostics, Indianapolis, IN). The homogenate was then spun at 1300 x g for 3 min and supernatant was collected. Following a second wash and spin at 1300 x g for 3 min, the supernatants were pooled and spun at 21,000 x g for 10 min. Synaptic and non-synaptic mitochondria were isolated using Percoll density gradient centrifugation as described previously [43]. Following isolation, pelleted mitochondria were resuspended in 1x mitochondrial assay solution (1x MAS; 70 mM sucrose, 220 mM mannitol, 10 mM KH_2PO_4, 5 mM $MgCl_2$, 2 mM HEPES, 1 mM EGTA, pH 7.2). The isolated mitochondrial protein concentrations were determined using the Pierce BCA Protein Assay Kit (Thermo Fisher Scientific, Waltham, MA) and used immediately for bioenergetic analysis or lysed in 4% SDS/DTT and stored at -80°C. Protein quantification prior to protein digestion for mass spectrometry was performed using a Pierce 660 nm Protein Assay with BSA standards with the addition of the ionic detergent compatibility reagent (IDCR, Thermo Fisher Scientific).

Bioenergetic analysis of isolated brain mitochondria

The isolated synaptic and non-synaptic mitochondria were assessed functionally using the Seahorse XF24 analyzer based on the protocol of Rogers [44] with minor alterations as described previously [45]. For the Seahorse experiments, synaptic and non-synaptic mitochondria isolated from three mice per strain (WT and htau) at each of the two ages (5 and 8 months) were utilized for the coupling assay. Each biological replicate ($n = 3$) had three to four technical replicate wells for the experiment.

Mass spectrometry-based proteomics

Protein digestion

Mouse synaptic and non-synaptic mitochondrial protein sample aliquots (35 µg) used for data-independent acquisition mass spectrometry were digested with trypsin using filter aided sample preparation [46]. The resultant peptides were desalted using Oasis mixed-mode weak cation exchanges cartridges (Waters, Milford, VA), dehydrated with a Savant ISS 110 SpeedVac concentrator (Thermo Fisher Scientific) and resuspended in 10 µL of 0.1% formic acid prior to quantification using a NanoDrop

2000 UV-vis spectrophotometer (Thermo Fisher Scientific) in conjunction with the Scopes method for peptide quantification by absorbance at 205 nm [47].

SWATH-MS analysis

The samples of peptides (2 µg) from WT and htau mouse synaptic and non-synaptic mitochondrial lysates were analyzed in triplicate (three biological replicates per strain (WT and htau, $n = 3$) by nano-LC-MS/MS in SWATH-MS mode on the 5600 TripleTOF instrument (SCIEX) and targeted data extraction was performed as previously described [43, 45]. All fragment ion chromatograms were extracted and automatically integrated with PeakView software (Version 2.1, SCIEX, Framingham, MA). For peptide identification, our published reference spectral library was used [43, 45]. This library was generated in ProteinPilot (Version 4.5, SCIEX) using the Paragon algorithm and the default settings. All searches were performed against the UniProt Mus Musculus Proteome UP000000589 containing 17,048 reviewed proteins (Swiss-Prot). Combined results yielded a library of 4,227 proteins identified with high confidence (greater than 99%) that passes the global FDR from fit analysis using a critical FDR of 1%. In accordance with previously published work [43, 45], we selected five peptides and five transitions option for quantitative analysis and performed targeted data extraction for each peptide. For each peptide, the fragment ion chromatograms were extracted using the SWATH isolation window set to a width of 10 min and 50 ppm accuracy [43, 45]. To calibrate retention times, synthetic peptides (Biognosys AG, Schlieren, Switzerland) were spiked-in to the samples in accordance with the manufacturer's protocol. Data were normalized to the median peak ratios of common proteins in MarkerView software (Version 1.2.1, SCIEX).

Bioinformatics

The Cyber-T Web server (http://cybert.ics.uci.edu/) [48], which implements a t-test using a Bayesian regularization method was used to assess statistical significance [49]. Proteins deemed as differentially expressed were p-values < 0.05 from the pairwise post-hoc test (TukeyHSD) that also exhibited Benjamini and Hochberg (BH) q-values < 0.05 to correct for multiple testing. The Search Tool for the Retrieval of Interacting Genes/Proteins (STRING [50]; https://string-db.org) was used to gain further insight into the role of the differentially expressed proteins via network clustering and functional annotation. Log_2-fold data obtained from the SWATH-MS analysis was clustered heirarchically between genotypes and withing genotypes between ages, using a Multiple Experiment Viewer (MEV, http://mev.tm4.org/, [51]) using the HCL method with a Eucleidian distance metric and complete linkage. Heatmaps were generated in GraphPad 9.

Western blot analysis

Biochemical isolation of synaptic mitochondrial isolates

For mitochondrial membrane protein analysis 60 µg of percoll isolated mitochondria were resuspended in 1 mL of 0.1 M Na_2CO_3, pH 11.5, and incubated on ice for 30 min. Following the incubation period samples were subjected to ultra-centrifugation at 100,000 x g for 20 min. The insoluble membrane fraction (pellet) solubilized by sonication and boiling at 95°C for 5 min in 30 µL solubilization buffer (SB;

100 mM Tris-HCl pH 7.4, 100mM DTT, 4% w/v SDS). The soluble protein fraction (supernatant) was concentrated by centrifugation with an Omega NanoSep 30K NWCO spin-filter (Pall, Port Washington, NY) at 14,000 x g until near dryness. Proteins were collected from spin-filters by pipette after the addition of 30 µL SB. The soluble protein fraction was then boiled at 95°C 5 min and sonicated briefly. Soluble and insoluble fractions were quantified using the Pierce 660 nm Protein Assay (Pierce) with the IDCR (Thermo Fisher Scientific). Equal masses of soluble and insoluble were analyzed by Western Blot.

Protease treatment of isolated mitochondria

Synaptic and non-synaptic mitochondria from 8 month old male htau mice were isolated by Percoll gradient as described above and final pellets were resuspended in 200 µL of 1x MAS and protein content was determined by Pierce 660 nm protein assay. 20 µg of total mitochondria were plated in each of 7 wells in a round bottom 96 well plate on ice in a total volume of 15 µL. Protease digests were started by the addition 15 µL of Trypsin diluted in 1x MAS to yield the final working concentration indicated in Fig. 5. Plates were incubated on ice for 30 min and mixed by gentle pipetting every 10 min. Once 30 min had passed protease action was halted by the addition of 2 µL of 200 mM phenylmethylsulfonyl fluoride, followed by gently pipette mixing and an additional incubation of 10 min on ice. SDS-Page samples were prepared by the addition of 10 µL of 4x sample buffer (Licor, Lincoln, NE), transfer to PCR strips tubes and boiling for 5 min st 95°C. Equal volumes of each sample were then resolved by SDS-Page, transferred to nitrocellulose and immunoblotted as described below with the indicated primary antibodies. Quantification was carried out by densitometric measurements made in Light Studio (Licor).

Immunoblot analysis

Isolated mitochondria were lysed in 4% SDS and protein quantification was performed using a Pierce 660 nm Protein Assay with BSA standards with the addition of the IDCR (Thermo Fisher Scientific). 10 µg of lysate was resolved on Nu-PAGE Bolt 4–12% gradient polyacrylamide gels gels using the MES/SDS buffer system (Life Technologies, Carlsbad, CA), transferred to nitrocellulose using an iBlot2 instrument (Invitrogen, Carlsbad, CA). Membranes were blocked with TBS/SuperBlock (Thermo Fisher Scientific) for 30 min at room temperature, and then probed with the indicated antibodies at appropriate dilutions (see Antibodies section) in Tris buffered saline with 0.1% Tween-20 (TBS-T)/SuperBlock and incubated overnight at 4°C. Blots were washed 3 x 10 min with 1x TBS-T and then incubated with appropriate secondary antibodies (Licor) for 1 hour at room temp. Membranes were again washed 3 x 10 min with 1x TBS-T and imaged using an Odyssey imager (Licor) using appropriate channels. Quantification of immunoreactivity was achieved using Image Studio software (Licor).

Statistical analysis

All experiments were conducted with a minimum of 3 biological replicates with or without 3–4 technical replicates (Seahorse only), and statistical analysis was performed using built-in analysis functions in Prism 9 (GraphPad, San Diego, CA). Statistical analysis of the SWATH analysis was determined by Cyber-T. The statistical tests performed are indicated in the figure legends.

Results

Synaptic mitochondria isolated from mice expressing non-mutant human tau isoforms exhibit age-associated bioenergetic alterations

To explore whether alterations in mitochondrial bioenergetics are involved in tauopathy pathogenesis, non-synaptic and synaptic mitochondria were isolated from htau transgenic and WT mice at 5- and 8-months of age and oxygen consumption rates (OCR) driven by complex II were measured utilizing the coupling assay [44]. Non-synaptic mitochondria from htau mice did not show alterations in respiration compared to WT mice at either age examined (Fig. 1A). Synaptic mitochondria isolated from htau mice at 8- (but not 5-) months of age exhibit a significant increase in the rate of complex II driven state 2 (basal), state 3 (ADP-stimulated), and state 3u (maximum uncoupled) respiration compared to those from age-matched WT mice (Fig. 1B). Tau pathology has been described in the brain of htau mice at 8-months [38], thus, mitochondria from the synapse are particularly sensitive to pathologic tau accumulation, and exhibit functional changes reported during aging [45].

Quantitative mitochondrial proteomics reveals accumulation of tau in association with synaptic mitochondria

To explore the molecular mechanisms underlying altered synaptic mitochondrial respiration in the absence of respiratory changes in non-synaptic mitochondria, we investigated the influence of human tau expression in mice on brain mitochondria protein expression profiles using the quantitative mass spectrometry-based technique SWATH-MS [52]. Synaptic and non-synaptic mitochondria were isolated from 5- and 8-month-old htau transgenic and WT mice, and the proteome was analyzed. In total, 1,578 proteins were identified and the complete list of these proteins with quantitative values is provided in Additional File 1: Supplementary Table S1. SWATH sample replicates exhibited a high degree of correlation, suggesting there was minimal sample-to-sample variablity within groups (Additional File 2: Supplemental Figs. 1–4). To uncover which proteins were differentially expressed (DE; FDR $q < 0.05$) in mitochondria isolated from htau as compared to age-matched WT mice, we used a Bayesian regularized t-test analysis and multiple testing corrections, which revealed 20 (5-months) and 12 (8-months) DE proteins in non-synaptic mitochondria samples, and 54 (5-months) and 31 (8-months) DE proteins in synaptic mitochondria samples (Additional File 1: Supplementary Table S2A-D). As shown in Fig. 2A, only 1 protein (Dephospho-CoA kinase domain containing protein (Dcakd)) was found to be DE in both non-synaptic and synaptic mitochondria isolated from 5-month old htau mice (as compared to age-matched WT mice), whereas 2 proteins (Mapt (tau) and tubulin alpha-4 chain (Tuba4a)) were found to be DE in synaptic mitochondria isolated from 5- and 8-month old htau mice (as compared to age-matched WT mice). Dcakd was found to be elevated in isolated non-synaptic and synaptic mitochondria from htau mice as compared to WT mice at 5-months (Fig. 2B). However, at 8-months, the levels of Dcakd are similar in isolated mitochondria between htau and WT mice. While Mapt (tau) levels are increased in isolated synaptic mitochondria from htau mice as compared to WT mice at both ages (Fig. 2C), Tuba4a is decreased at 5-months and increased at 8-months (Fig. 2D). Of note, Mapt (tau) levels are increased in

isolated mitochondria from 8- as compared to 5-month-old htau mice, highlighting an age-dependent increase.

To uncover protein-protein interaction networks and perform enrichment analysis to gain insight into functional associations of the mitochondrial protein changes, the lists of DE proteins in htau versus age-matched WT mice for each mitochondrial population (non-synaptic and synaptic mitochondria) were uploaded to the STRING database. Only interactions which were of high confidence (minimum required interaction score of 0.07) were used to generate the interaction networks using the MCL clustering method (network clusters are denoted by node color). This analysis identified 8 interacting proteins organized in 4 networks for the 5-month non-synaptic mitochondria DE proteins (Fig. 3A), 2 proteins organized in 1 network for the 8-month non-synaptic mitochondria DE proteins (Fig. 3B), 29 interacting proteins organized in 7 networks with 9 distinct network clusters for the 5-month synaptic mitochondria DE proteins (Fig. 3C), and 13 interacting proteins organized in 3 networks for the 8-month synaptic mitochondria DE proteins (Fig. 3D). While the networks for the non-synaptic mitochondria DE proteins were composed of single interactions between 2 proteins, the networks for the synaptic mitochondria DE proteins were more complex, evidenced by the increased numbers of nodes and edges. Functional enrichments in the STRING networks revealed gene ontology (GO) biological process (BP) terms that were altered according to our proteomics results (Additional File 1: Supplementary Table S3A-C). While no BP terms were identified for the 5-month non-synaptic mitochondria, one term was found for the DE proteins in non-synaptic mitochondria from 8-month htau compared to WT mice were “positive regulation of hydrolase activity” (FDR = 0.0078). In contrast, several BP terms (131 at 5-months and 9 at 8-months) were significantly enriched based on the DE proteins in synaptic mitochondria from htau as compared to WT mice, with the top two terms “synaptic vesicle docking” and “glycerol-3-phosphate metabolic process” at 5-months, and “microtubule-based process” and “cytoskeleton organization” at 8-months. Of note, Mapt (tau) was a node in the STRING networks for synaptic mitochondria DE proteins at both ages studied.

Human tau expression alters expression of electron transport chain components

To determine whether proteomic changes affecting the electron transport chain (ETC) and oxidative phosphorylation (OxPhos) correlate with the observed respiratory alterations, we assessed the expression of the ETC component proteins as well as regulators of complex assembly and function (Fig. 4). We used the web served based MEV to cluster $\log_2$-fold expression data comparing synaptic and non-synaptic data between htau and WT mice at 5- and 8-months of age (Fig. 4A). Clustering indicated that expression changes in ETC components were most similar between synaptic and non-synaptic mitochondria a 5-months. Furthermore, changes 8-month synaptic mitochdonria were the most divergent between genotypes, a finding that correlates well with the changes we observed in bioeneregetics of 8-month synaptic mitochondria. Interestingly, the age-dependent alterations of mitochondrial respiratory complex subunit expression in synaptic mitochondria from WT mice were similar to changes observed in htau transgenic mice consistent with the observation of similar synaptic mitochondrial functional alterations with age in htau transgenic and WT mice. However, despite the predominant conservation of age-

dependent changes in the synaptic mitochondrial ETC subunits and regulator proteins in htau mice, differences exist which may contribute to the functional differences between htau and WT mice at 8-months of age. Therefore, we focused on the synaptic mitochondrial proteomic changes between htau and WT mice at 8-months of age to gain mechanistic insight into the contribution of tau pathology to alterations in synaptic mitochondrial function. Upon examination of the differences in the expression of the ETC subunits between 8-month-old htau and WT mice it becomes apparent that several of the mitochondrial DNA (mtDNA) encoded subunits (Mtnd4 (log2 = -1.43), Mtnd5 (log2 = 1.10), and Mtco1 (log2 = -0.176)) exhibit altered expression (Additional File 1: Supplementary Table 1, Fig. 4A (red row names)). Although not reaching significance in our proteomic analysis due to the stringency of our statistical analysis, lower Mtco1 levels were confirmed via immunoblotting (Fig. 4B). Similar to Mtco1, our proteomic analysis revealed a slight reduction in Uqcrc2 expression in synaptic mitochondria from 8-month-old htau compared to WT mice (log2 = -0.256), which was confirmed by immunobot quanitfication (Supplementary Table 1; Fig. 4). A similar observation was made for Atp5a1 (log2 = -0.44). Since htau mice exhibit hyperphosphorylation and aggregation of tau within the span from 5- to 8-months of age [38], we next sought to characterize tau associated with synaptic mitochondria as our functional and proteomic results suggested this popoulation of mitochondria was the most divergent.

Accumulation of pathologic tau in association with synaptic mitochondria

Phosphorylation of tau at certain serine and threonine residues serves as a biochemical marker for pathologic alterations in AD and fronto-temporal dementia (FTD) [2, 10, 26, 36, 38]. We therefore sought to determine whether alterations in synaptic mitochondrial bioenergetics were associated with this hallmark of disease progression. We used immunoblotting to determine if tau was present in purified synaptic mitochondrial isolates (Fig. 5). In agreeance with our SWATH analysis (Fig. 2) we observed a significant increase in the amount of total tau protein present in htau mice at both 5- and 8-months of age compared with WT mice, which was more pronounced at 8 compared to 5 months of age (Fig. 5A). We also detected CP13 [8, 9, 53] and PHF1 [54, 55] positive immunoreactivity in isolated synaptic mitochondria, which specifically detect abnormal phosphorylated residues S202 (Fig. 5B) and S396/404 (Fig. 5C), respectively. In synaptic mitochondria we observed low but comparable levels of CP13 immunoreactivity between 5-month-old WT and htau mice, however, at 8-months we detected a significant increase of CP13 signal in synaptic mitochondria from htau mice (Fig. 5B). In contrast to CP13, we detected a significant increase in PHF1 signal at both 5- and 8-months in synaptic mitochondria from htau mice as compared to WT, and this exaggerated at 8-months (Fig. 5C). In addition to pathologic hyperphosphorylation, tau also changes its conformation during disease progression [56], which finally culminates in aggregation and formation of tangles. These early conformational changes can be monitored by probing with the antibody MC1, which is specific for a pathologic conformation of tau as it recognizes neurofibrillary tangles (NFTs) [56]. In synaptic mitochondria from 5-month-old htau mice there was a trending albeit insignificant increase in MC1 signal that achieved significance at 8-months (Fig. 5D). Interestingly, a significant increase in the detection of PFH1 tau was observed at both 5- and 8-months timepoints, suggesting increased phosphorylation at S396/404 may be an earlier event in the progression of AD and related tauopathies (Fig. 5C).

Tau localizes to the mitchondrial outer membrane

Other studies have reported the association of tau protein with mitochondria in a number of systems [11, 13, 28, 36, 57–59]. This association was determined in some cases to be the result of tau incorporation into the outer mitochondrial membrane, yet in others the consequence of protein-protein interactions with outer mitochondrial membrane proteins, one such protein is voltage dependent anion channel 1 (VDAC1) [60–63]. With this in mind we sought to determine the mechanism by which tau was co-purifying with synaptic mitochondria in our isolations. To address this, we used sodium carbonate extraction, an established method to differentiate integral mitochondrial membrane proteins from membrane associated mitochondrial proteins. In this assay integral membrane proteins fractionate into an insoluble (pellet; “P”) fraction, while peripheral membrane (i.e. membrane associated) proteins segregate into the soluble (“S”) fraction. Synaptic mitochondria isolated from 8-month-old htau mice were extracted with sodium carbonate and the resulting fractions were probed by western blot (Fig. 6). As control we probed for the OxPhos panel (Fig. 6A, red) as well as heat-shock protein 60 (HSP60) (Fig. 6A, green). With the exception of ATP synthase F1 subunit alpha (Atp5a1), we primarily detected the proteins of the OxPhos panel in the pellet as expected since most are integral membrane proteins, also as expected we observed the majority of HSP60 in the soluble fraction. Finally, we observed tau protein segregating almost entirely into the soluble fraction (Fig. 6B). Our results suggest that tau associated with synaptic mitochondria is not inserted into the mitochondrial membrane, but likely associated via protein-protein interaction.

To further support our sodium carbonate extraction results, we employed a protease digest assay to determine the rate at which tau was degraded compared to two mitochondrial proteins. We reasoned that if tau was associated with mitochondria via protein-protein interactions it would be degraded at lower concetrations of protease than either integral membrane or mitochondrial matrix proteins. Isolated synaptic and non-synpatic mitochondria from approximately 8-month-old htau mice were digested by trypsin and immunoblotted for tau, VDAC, and succinate dehydrogenase complex subunit A (SDHA) (Fig. 6C). We observed a reduced percentage of remaining full length tau protein at lower trypsin concentration than either SDHA or VDAC, suggesting mitochondrially associated tau is more accessible to proteolytic action. Taken together with our sodium carbonate extraction results, this suggests that tau is present on the mitochondrial outer membrane and this interaction is most likely mediated by protein-protein interactions.

Discussion

Tau impairs synaptic bioenergetics and alters electron transport chain subunit expression

We compared the bioenergetic profiles of synaptic and non-synaptic mitochondria and observed an age- and pathological tau-dependent shift in the bioenergetics of synaptic mitochondria only. Specifically, we determined a significant elevation in both basal and maximal respiration in synaptic mitochondria from aged htau mice that was not observed in the young or aged WT controls, nor young htau cohorts. Interestingly, despite elevated basal and maximal respiratory capacity the spare respiratory capacity

(SRC) in these mitochondria was impaired. These changes are characteristic of an aged synaptic mitochondrial bioenergetic phenotype, which we previously reported in WT mice [45]. Further, we observed similar age-dependent complex II changes in the Pink1 KO rat model of Parkinson's disease (PD) [64], which in striatal synaptic mitochondria was accompanied by decreased complex I respiration. Studies in other systems have reported similar findings. For example, Flynn *et al* [65], observed an impaired SRC in synaptosomes isolated from super-oxide dismutase 2 (SOD2) null mice, which have been reported to mimic tauopathies by accumulation of amyloid and tau deposits [66–70]. Another study reported that genetic ablation of tau expression improved hippocampal mitochondrial function despite reducing expression of proteins of the ETC [71]. Furthermore, studies investigating pathological mutant forms of tau have similarly reported alterations is bioenergetic. One such study by David *et al*, demonstrated expression if P301L mutant tau in mice resulted in impaired respiratory control ratio and ATP production from cerebral mitochondrial isolates [72]. Notably, the authors also reported increased reactive oxygen species (ROS) production and SOD activity supporting the notion that increased oxidative states promote tauopathy [72]. Several studies have reported increased ROS production as a consequence of complex II driven respiration [73–75]. One such study of isolated mitochondria from rat skeletal muscle reported high rates of H_2O_2 production driven by complex II when complex I and III were inhibited [73]. Furthermore, inhibition of complex II by either malonate or malate completely abrogated H_2O_2 production [73]. A similar observation was reported in rat cardiac mitochondria [74]. In our assessment of bioenergetics, we observed elevated complex II driven respiration in the synaptic mitochondria from 8-month htau mice compared to WT, suggesting that an increase in ROS may similarly contribute to pathology in our system. Indeed elevated ROS has also been reported in models of AD [68, 76–78], as well as samples from AD patients [79, 80].

In line with our observations that the bioenergetics of synapses (i.e. synaptic mitochondria) are altered by the accumulation of pathological forms of tau protein we observed changes in the expression of components of the ETC including Mtco1. Interestingly, other reports have suggested that reduction of Mtco1 expression is positively selected for as cells trend towards mitochondrial homoplasmy [81]. Notably, decreased expression of Mtco1 correlates with reduced generation of ROS and improved cell survival via impaired apoptosis [81]. Taken together this may suggest a potential mechanism by which early tau accumulation serves a neuroprotective role by reduction of Mtco1 expression. In addition to alterations in Mtco1 expression we observed a decrease in Mtnd4 expression. Mtnd4 is principle component of the minimal assembly core for mitochondrial complex I, and is critical for proper ETC function [82]. Importantly, impaired complex I function has been been reported in several neurodegenerative disorders including PD [83, 84] and altered expression of complex I subunit proteins has been reported in AD [85, 86]. Recently, a study investigating global proteomic changes reported altered expression of a number of mitochondrial proteins in AD patient brain regions in early and late stages of disease [86]. Notably, expression of several mitochondrial proteins was observed to decrease, specifically in the entorhinal and parahippocampal cortices, two regions known to be affected by AD [86–88]. Furthermore, the study reported a decrease in the expression of Mtnd4 and Mtnd1 in late stage AD [86]. Although, we did not observe a significant difference in the expression of Mtnd1, we did observe a

significant decrease in expression of Mtnd4. Possible explanations for this difference could be the larger group size in the study by Mendonça *et al.*, or intrinsic differences between humans and mice neurophysiology. Another likely contributor to the differences between our study and that of Mendonça is our use of rather strict statistical analysis, which results in increased confidence of our results, could also result in Type II error (not achieving statistical significance despite being differentially expressed). Of note our analysis did reveal a trending, albeit not significant, decrease in the expression of Mtnd1 in isolates of synaptic mitochondria at 8-months between WT and htau mice. Nevertheless, the congurencies in our analysis and that of Mendonça lends support to the validity of both our study as well as use of the htau model in studying the pathogenesis of AD.

Pathological forms of tau accumulate with synaptic mitochondria

We observed significant increases in the accumulation of total tau protein as well as pathological forms of the protein (including hyperphosphorylated and NFTs). A number of studies have reported the accumulation of these species in the brains of AD patients and models of AD and related tauopathies [2, 8, 27, 38, 54, 89]. One study from 2008, reported the accumulation of tau protein in synaptosomes isolated from brains perimortem, where it colocalized with amyloid [90]. Furthermore, using immunofluorescent imaging hyper-phosphorylated tau was observed to primarily in neurites of intact neurons [90]. In another study of postmortem dementia patient samples, synaptic accumulation of both total and hyper-phosphorylated tau was reported in conjunction with ubiquitin-proteosome dysfunction [91]. Indeed, other studies have demonstrated the accumulation of tau impaired mitophagy by protecting the mitochondrial membrane potential to prevent activation of the Pink1/Parkin pathway [57] or by sequestration of cytosolic Parkin preventing its recruitment to damaged mitochondria [92]. Although they did not investigate synaptic accumulation of tau specifically, Cook *et al* injected neonatal mice with AAV-Tau^{P301L} on day P0 and observed significant widespread accumulation of tau protein and NFTs in these mice by 6 months of age [93]. Tau accumulation in these animals correlated with increased neuroinflammation and cognitive deficits [93]. Conversely, Sahara *et al*, reported no preferential synaptic accumulation of tau^{P301L} in transgenic mice [94]. They did however note, that tau protein contained within the synaptosomal fraction appeared to be membrane associated [94]. Furthermore, in contrast to our findings, the author's observed a decrease in the relative amount of tau phosphorylation in synaptic membrane fractions [94]. A study in Drosophila reported tau localization and accumulation in pre-synaptic terminals and similarly to Sahara *et al.*, it was demonstrated to associate with the pre-synaptic membrane [95]. Our results suggest there may exist an alternate mechanism by which tau accumulates in the pre-synaptic terminal by preferentially associating with mitochondrial membranes. Future studies that focus on determining mechanistically how tau preferentially associates with synaptic mitochondria will be of significant interest.

Conclusions

In the current study we have reported that pathological forms of tau protein accumulate and associate with synaptic mitochondria and impair synaptic bioenergetics. Our study highlights the importance of

techniques used to separate unique populations of cells or organelles. While our results indicate tau accumulation is more detrimental to the function of synaptic mitochondria, the precise molecular mechanisms that govern preferential associations between tau and synaptic mitochondria remain elusive, and thus should be the subject of detailed future investigations.

Abbreviations

AAV – Adeno-associated virus

AD – Alzheimer's Disease

ATP – Adenosine triphosphate

Atp5a1 – ATP synthase F1 subunit alpha

BH – Benjamini-Hochberg

BP – Biological process

Dcakd - Dephospho-CoA Kinase Domain Containing protein

DE – Differentially expressed

ETC – Electron transport chain

FDR – False discovery rate

FTD – Fronto-temporal dementia

GO – Gene Ontology

HSP60 – Heat-shock protein of 60 kDa

IDCR – Ionic detergent compatibility reagent

KO – Knock-out

Map – Microtubule-associated protein

Mapt – Microtubule-associated protein tau

MAS – Mitochondrial assay solution

MEV – Multiple Experiment Viewer

MS – Mass spectrometry

MSHE – Mitochondrial isolation buffer (Mannitol, sucrose, HEPES, EGTA)

MT – Microtubule

Mtco1 - Mitochondrially encoded cyctochrome c oxidase 1

Mtnd – Mitochondirally encoded NADH dehydrogenase

NFT – Neurofibrillary tangles

OxPhos – Oxidative phosphorylation

P – Pellet

PD – Parkinson's Disease

PHF – Paired helical fragment

ROS – Reactive oxygen species

S – Soluble

SB – Solubilization buffer

SDHA – Succinate dehydrogenase complex subunit A

SRC – Spare respiratory capacity

STRING – Search Tool for the Retrieval of Interacting Genes/Proteins

SWATH-MS – Sequential Window Acquisition of all Theoretical Mass Spectra

Syn – Synaptic

Tuba4a – Tubulin alpha 4a

Uqcrc2 – Ubiquinol-cytochrome c reductase core protein 2

VDAC – Voltage dependent anion channel

WT – Wild-type

Declarations

Funding

This work was supported by a National Institutes of Health grants from the National Institute on Aging (award number R01AG059785 to KLS) and the National Institute of Mental Heath (award number P30 MH062261 to HSF).

Availability of data and materials

The datasets generated and analyzed during the current study are available from the corresponding author upon request.

Competing interests

The authors declare that they have no competing interests.

Authors' contributions

The authors have made the following declarations about their contributions: Conceived and designed the experiments: KS, HF. Performed the experiments: KS, KE, AT. Analyzed the data: KS, KE, AT, JG. Wrote the paper: KS, HF, AT, JG, KE. All authors read and approved the final manuscript.

Acknowledgements

We would like to acknowledge the UNMC Mass Spectrometry and Proteomics Core Facility and the UNMC Seahorse Core Facility and their staff for their assistance in data acquisition and analysis. The University of Nebraska Medical Center Mass Spectrometry and Proteomics Core Facility is administrated through the Office of the Vice Chancellor for Research and supported by state funds from the Nebraska Research Initiative (NRI). We would also like to thank Peter Davies (Feinstein Institute for Medical Research, Manhasset, NY) for his generous gift of the pathological tau antibodies (MC1, PHF1, and CP13).

Author Details

[†]Department of Neurological Sciences, University of Nebraska Medical Center, Omaha, NE, USA

References

1. Stelzmann RA, Norman Schnitzlein H, Reed Murtagh F. An english translation of Alzheimer's 1907 paper, "über eine eigenartige erkankung der hirnrinde." Clin Anat. 1995;8:429–31.
2. Thompson PM, Vinters H V. Pathologic lesions in neurodegenerative diseases. In: Progress in Molecular Biology and Translational Science. Elsevier B.V.; 2012. p. 1–40. doi:10.1016/B978-0-12-385883-2.00009-6.
3. Ower AK, Hadjichrysanthou C, Gras L, Goudsmit J, Anderson RM, de Wolf F. Temporal association patterns and dynamics of amyloid-$β$ and tau in Alzheimer's disease. Eur J Epidemiol.

2018;33:657–66.

4. Franzmeier N, Neitzel J, Rubinski A, Smith R, Strandberg O, Ossenkoppele R, et al. Functional brain architecture is associated with the rate of tau accumulation in Alzheimer's disease. Nat Commun. 2020;11:1–17.
5. Serrano-Pozo A, Frosch MP, Masliah E, Hyman BT. Neuropathological alterations in Alzheimer disease. Cold Spring Harb Perspect Med. 2011;1.
6. Nelson PT, Alafuzoff I, Bigio EH, Bouras C, Braak H, Cairns NJ, et al. Correlation of Alzheimer Disease Neuropathologic Changes With Cognitive Status: A Review of the Literature NIH Public Access. J Neuropathol Exp Neurol. 2012;71:362–81.
7. Jung Y, Whitwell JL, Duffy JR, Strand EA, Machulda MM, Senjem ML, et al. Regional β-amyloid burden does not correlate with cognitive or language deficits in Alzheimer's disease presenting as aphasia.
8. Koss DJ, Dubini M, Buchanan H, Hull C, Platt B. Distinctive temporal profiles of detergent-soluble and -insoluble tau and A$β$ species in human Alzheimer's disease. Brain Res. 2018;1699:121–34.
9. Lewis J, McGowan E, Rockwood J, Melrose H, Nacharaju P, Van Slegtenhorst M, et al. Neurofibrillary tangles, amyotrophy and progressive motor disturbance in mice expressing mutant (P301L)tau protein. Nat Genet. 2000;25:402–5. doi:10.1038/78078.
10. Jose Metcalfe M, Figueiredo-Pereira ME, Sinai Med Author manuscript MJ. Relationship Between Tau Pathology and Neuroinflammation in Alzheimer's Disease NIH Public Access Author Manuscript. Mt Sinai J Med. 2010;77:50–8.
11. Vossel KA, Zhang K, Brodbeck J, Daub AC, Sharma P, Finkbeiner S, et al. Tau Reduction Prevents Aβ-Induced Defects in Axonal Transport. doi:10.1126/science.1194653.
12. Roberson ED, Scearce-Levie K, Palop JJ, Yan F, Cheng IH, Wu T, et al. Reducing endogenous tau ameliorates amyloid β-induced deficits in an Alzheimer's disease mouse model. Science (80-). 2007;316:750–4. doi:10.1126/science.1141736.
13. Rhein V, Song X, Wiesner A, Ittner LM, Baysang G, Meier F, et al. Amyloid-$β$ and tau synergistically impair the oxidative phosphorylation system in triple transgenic Alzheimer's disease mice. Proc Natl Acad Sci U S A. 2009;106:20057–62.
14. Ittner LM, Ke YD, Delerue F, Bi M, Gladbach A, van Eersel J, et al. Dendritic function of tau mediates amyloid-$β$ toxicity in alzheimer's disease mouse models. Cell. 2010;142:387–97.
15. Shahpasand K, Uemura I, Saito T, Asano T, Hata K, Shibata K, et al. Regulation of mitochondrial transport and inter-microtubule spacing by tau phosphorylation at the sites hyperphosphorylated in Alzheimer's disease. J Neurosci. 2012;32:2430–41.
16. Llorens-Martín M, Ló Pez-Doménech G, Soriano E, Avila JS. GSK3b Is Involved in the Relief of Mitochondria Pausing in a Tau-Dependent Manner. PLoS One. 2011;6:27686. doi:10.1371/journal.pone.0027686.
17. Kopeikina KJ, Carlson GA, Pitstick R, Ludvigson AE, Peters A, Luebke JI, et al. Tau accumulation causes mitochondrial distribution deficits in neurons in a mouse model of tauopathy and in human

Alzheimer's disease brain. Am J Pathol. 2011;179:2071–82.

18. Hernandez F, Arai T, Kametani F, Hasegawa M. Reconsideration of Amyloid Hypothesis and Tau Hypothesis in Alzheimer's Disease. Front Neurosci | www.frontiersin.org. 2018;1. doi:10.3389/fnins.2018.00025.
19. Kadavath H, Hofele R V, Biernat J, Kumar S, Tepper K, Urlaub H, et al. Tau stabilizes microtubules by binding at the interface between tubulin heterodimers. doi:10.1073/pnas.1504081112.
20. Rodríguez-Martín T, Cuchillo-Ibáñez I, Noble W, Nyenya F, Anderton BH, Hanger DP. Tau phosphorylation affects its axonal transport and degradation. Neurobiol Aging. 2013;34:2146–57. doi:10.1016/j.neurobiolaging.2013.03.015.
21. Venkatramani A, Panda D. Regulation of neuronal microtubule dynamics by tau: Implications for tauopathies. International Journal of Biological Macromolecules. 2019;133:473–83. doi:10.1016/j.ijbiomac.2019.04.120.
22. Lacovich V, Espindola SL, Alloatti M, Pozo Devoto V, Cromberg LE, C ˇ arná ME, et al. Neurobiology of Disease Tau Isoforms Imbalance Impairs the Axonal Transport of the Amyloid Precursor Protein in Human Neurons. 2017.
23. Avila J, Jadhav S, Primio C Di, Devred F, Landrieu I, Barbier P, et al. Role of Tau as a Microtubule-Associated Protein: Structural and Functional Aspects. 2019. doi:10.3389/fnagi.2019.00204.
24. Kanaan NM, Morfini GA, Lapointe NE, Pigino GF, Patterson KR, Song Y, et al. Neurobiology of Disease Pathogenic Forms of Tau Inhibit Kinesin-Dependent Axonal Transport through a Mechanism Involving Activation of Axonal Phosphotransferases. 2011.
25. Morris M, Maeda S, Vossel K, Mucke L. The Many Faces of Tau A Microtubule-associated Protein Involved in Disease. 2011. doi:10.1016/j.neuron.2011.04.009.
26. Grundke-Iqbal I, Iqbal K, Tung YC, Quinlan M, Wisniewski HM, Binder LI. Abnormal phosphorylation of the microtubule-associated protein tau (tau) in Alzheimer cytoskeletal pathology. Proc Natl Acad Sci U S A. 1986;83:4913–7.
27. Despres C, Byrne C, Qi H, Cantrelle FX, Huvent I, Chambraud B, et al. Identification of the Tau phosphorylation pattern that drives its aggregation. Proceedings of the National Academy of Sciences of the United States of America. 2017;114:9080–5.
28. Cieri D, Vicario M, Vallese F, D'Orsi B, Berto P, Grinzato A, et al. Tau localises within mitochondrial sub-compartments and its caspase cleavage affects ER-mitochondria interactions and cellular Ca 2+ handling. Biochim Biophys Acta - Mol Basis Dis. 2018;1864:3247–56.
29. Article R. SYNAPTIC NEUROSCIENCE. Article. 2010;2. doi:10.3389/fnsyn.2010.00139.
30. Sheng Z-H, Cai Q. Mitochondrial transport in neurons: impact on synaptic homeostasis and neurodegeneration HHS Public Access. 2016. doi:10.1038/nrn3156.
31. Harada A, Oguchi K, Okabe S, Kuno J, Terada S, Ohshima T, et al. Altered microtubule organization in small-calibre axons of mice lacking tau protein. Nature. 1994;369:488–91. doi:10.1038/369488a0.

32. Dawson HN, Ferreira A, Eyster M V, Ghoshal N, Binder LI, Vitek MP. Inhibition of neuronal maturation in primary hippocampal neurons from τ deficient mice. J Cell Sci. 2001;114:1179 LP – 1187. http://jcs.biologists.org/content/114/6/1179.abstract.
33. Takei Y, Teng J, Harada A, Hirokawa N. Defects axonal elongation and neuronal migration in mice with disrupted tau and map1b genes. J Cell Biol. 2000;150:989–1000. doi:10.1083/jcb.150.5.989.
34. Liu CWA, Lee G, Jay DG. Tau is required for neurite outgrowth and growth cone motility of chick sensory neurons. Cell Motil Cytoskeleton. 1999;43:232–42. doi:10.1002/(SICI)1097-0169(1999)43:3<232::AID-CM6>3.0.CO;2-7.
35. Kanai Y, Takemura R, Oshima T, Mori H, Ihara Y, Yanagisawa M, et al. Expression of multiple tau isoforms and microtubule bundle formation in fibroblasts transfected with a single tau cDNA. J Cell Biol. 1989;109:1173–84. doi:10.1083/jcb.109.3.1173.
36. Zhang L-F, Shi L, Liu H, Meng F-T, Liu Y-J, Wu H-M, et al. Increased hippocampal tau phosphorylation and axonal mitochondrial transport in a mouse model of chronic stress. doi:10.1017/S1461145711000411.
37. Tracy TE, Gan L. Tau-mediated synaptic and neuronal dysfunction in neurodegenerative disease. Current Opinion in Neurobiology. 2018;51:134–8. doi:10.1016/j.conb.2018.04.027.
38. Andorfer C, Kress Y, Espinoza M, De Silva R, Tucker KL, Barde YA, et al. Hyperphosphorylation and aggregation of tau in mice expressing normal human tau isoforms. J Neurochem. 2003;86:582–90.
39. Khatoon S, Grundke-Iqbal I, Iqbal K. Levels of normal and abnormally phosphorylated tau in different cellular and regional compartments of Alzheimer disease and control brains. FEBS Lett. 1994;351:80–4. doi:10.1016/0014-5793(94)00829-9.
40. Menkes-Caspi N, Yamin HG, Kellner V, Spires-Jones TL, Cohen D, Stern EA. Pathological tau disrupts ongoing network activity. Neuron. 2015;85:959–66.
41. Kuznetsov IA, Kuznetsov AV. A coupled model of fast axonal transport of organelles and slow axonal transport of tau protein. Comput Methods Biomech Biomed Engin. 2015;18:1485–94. doi:10.1080/10255842.2014.920830.
42. Polydoro M, Acker CM, Duff K, Castillo PE, Davies P. Age-dependent impairment of cognitive and synaptic function in the htau mouse model of Tau pathology. J Neurosci. 2009;29:10741–9.
43. Stauch KL, Purnell PR, Fox HS. Quantitative proteomics of synaptic and nonsynaptic mitochondria: Insights for synaptic mitochondrial vulnerability. J Proteome Res. 2014;13:2620–36. doi:10.1021/pr500295n.
44. Rogers GW, Brand MD, Petrosyan S, Ashok D, Elorza AA, Ferrick DA, et al. High Throughput Microplate Respiratory Measurements Using Minimal Quantities Of Isolated Mitochondria. PLoS One. 2011;6:e21746. doi:10.1371/journal.pone.0021746.
45. Stauch KL, Purnell PR, Fox HS. Aging synaptic mitochondria exhibit dynamic proteomic changes while maintaining bioenergetic function. Aging (Albany NY). 2014;6:320–34. doi:10.18632/aging.100657.

46. Wiśniewski JR. Filter-Aided Sample Preparation: The Versatile and Efficient Method for Proteomic Analysis. In: Methods in Enzymology. Academic Press Inc.; 2017. p. 15–27. doi:10.1016/bs.mie.2016.09.013.
47. Scopes RK. Measurement of protein by spectrophotometry at 205 nm. Anal Biochem. 1974;59:277–82.
48. Kayala MA, Baldi P. Cyber-T web server: Differential analysis of high-throughput data. Nucleic Acids Res. 2012;40. doi:10.1093/nar/gks420.
49. Baldi P, Long AD. A Bayesian framework for the analysis of microarray expression data: Regularized t-test and statistical inferences of gene changes. Bioinformatics. 2001;17:509–19. doi:10.1093/bioinformatics/17.6.509.
50. Szklarczyk D, Franceschini A, Kuhn M, Simonovic M, Roth A, Minguez P, et al. The STRING database in 2011: Functional interaction networks of proteins, globally integrated and scored. Nucleic Acids Res. 2011;39 SUPPL. 1:D561. doi:10.1093/nar/gkq973.
51. Howe E, Holton K, Nair S, Schlauch D, Sinha R, Quackenbush J. MeV: MultiExperiment viewer. In: Biomedical Informatics for Cancer Research. Springer US; 2010. p. 267–77. doi:10.1007/978-1-4419-5714-6_15.
52. Gillet LC, Navarro P, Tate S, Röst H, Selevsek N, Reiter L, et al. Targeted data extraction of the MS/MS spectra generated by data-independent acquisition: A new concept for consistent and accurate proteome analysis. Mol Cell Proteomics. 2012;11. doi:10.1074/mcp.O111.016717.
53. Duff K, Knight H, Refolo LM, Sanders S, Yu X, Picciano M, et al. Characterization of pathology in transgenic mice over-expressing human genomic and cDNA tau transgenes. Neurobiol Dis. 2000;7:87–98. doi:10.1006/nbdi.1999.0279.
54. Otvos L, Feiner L, Lang E, Szendrei GI, Goedert M, Lee VM. Monoclonal antibody PHF-1 recognizes tau protein phosphorylated at serine residues 396 and 404. J Neurosci Res. 1994;39:669–73. doi:10.1002/jnr.490390607.
55. Greenberg SG, Davies P, Schein JD, Binder LI. Hydrofluoric acid-treated tau PHF proteins display the same biochemical properties as normal tau. J Biol Chem . 1992;267:564–9. http://www.jbc.org/content/267/1/564.abstract.
56. Jicha GA, Bowser R, Kazam IG, Davies P. Alz-50 and MC-1, a new monoclonal antibody raised to paired helical filaments, recognize conformational epitopes on recombinant tau. J Neurosci Res. 1997;48:128–32. doi:10.1002/(SICI)1097-4547(19970415)48:2<128::AID-JNR5>3.0.CO;2-E.
57. Hu Y, Li X-C, Wang Z-H, Luo Y, Zhang X, Liu X-P, et al. Tau accumulation impairs mitophagy via increasing mitochondrial membrane potential and reducing mitochondrial Parkin. 2016. www.impactjournals.com/oncotarget/. Accessed 9 May 2020.
58. Li XC, Hu Y, Wang ZH, Luo Y, Zhang Y, Liu XP, et al. Human wild-type full-length tau accumulation disrupts mitochondrial dynamics and the functions via increasing mitofusins. Sci Rep. 2016;6:1–10.
59. Zündorf G, Reiser G. Calcium dysregulation and homeostasis of neural calcium in the molecular mechanisms of neurodegenerative diseases provide multiple targets for neuroprotection.

Antioxidants and Redox Signaling. 2011;14:1275–88.

60. Reddy PH. Amyloid beta-induced glycogen synthase kinase 3β phosphorylated VDAC1 in Alzheimer's disease: Implications for synaptic dysfunction and neuronal damage. Biochimica et Biophysica Acta - Molecular Basis of Disease. 2013;1832:1913–21.
61. Quintanilla RA, Matthews-Roberson TA, Dolan PJ, Johnsion GVW. Caspase-cleaved tau expression induces mitochondrial dysfunction in immortalized cortical neurons: Implications for the pathogenesis of alzheimer disease. J Biol Chem. 2009;284:18754–66. doi:10.1074/jbc.M808908200.
62. Atlante A, Amadoro G, Bobba A, De Bari L, Corsetti V, Pappalardo G, et al. A peptide containing residues 26-44 of tau protein impairs mitochondrial oxidative phosphorylation acting at the level of the adenine nucleotide translocator. 2008.
63. Amadoro G, Corsetti V, Ciotti MT, Florenzano F, Capsoni S, Amato G, et al. Endogenous A causes cell death via early tau hyperphosphorylation. Neurobiol Aging. 2011;32:969–90.
64. Stauch KL, Villeneuve LM, Purnell PR, Ottemann BM, Emanuel K, Fox HS. Loss of Pink1 modulates synaptic mitochondrial bioenergetics in the rat striatum prior to motor symptoms: concomitant complex I respiratory defects and increased complex II-mediated respiration. Proteomics - Clin Appl. 2016;10:1205–17. doi:10.1002/prca.201600005.
65. Flynn JM, Choi SW, Day NU, Gerencser AA, Hubbard A, Melov S. Impaired spare respiratory capacity in cortical synaptosomes from Sod2 null mice. Free Radic Biol Med. 2011;50:866–73. doi:10.1016/j.freeradbiomed.2010.12.030.
66. Su B, Wang X, gon Lee H, Tabaton M, Perry G, Smith MA, et al. Chronic oxidative stress causes increased tau phosphorylation in M17 neuroblastoma cells. Neurosci Lett. 2010;468:267–71.
67. Stamer K, Vogel R, Thies E, Mandelkow E, Mandelkow EM. Tau blocks traffic of organelles, neurofilaments, and APP vesicles in neurons and enhances oxidative stress. J Cell Biol. 2002;156:1051–63. doi:10.1083/jcb.200108057.
68. Resende R, Moreira PI, Proença T, Deshpande A, Busciglio J, Pereira C, et al. Brain oxidative stress in a triple-transgenic mouse model of Alzheimer disease. Free Radic Biol Med. 2008;44:2051–7. doi:10.1016/j.freeradbiomed.2008.03.012.
69. Jiang T, Sun Q, Chen S. Oxidative stress: A major pathogenesis and potential therapeutic target of antioxidative agents in Parkinson's disease and Alzheimer's disease. Progress in Neurobiology. 2016;147:1–19. doi:10.1016/j.pneurobio.2016.07.005.
70. Melov S, Adlard PA, Morten K, Johnson F, Golden TR, Hinerfeld D, et al. Mitochondrial oxidative stress causes hyperphosphorylation of tau. PLoS One. 2007;2:536. doi:10.1371/journal.pone.0000536.
71. Jara C, Aránguiz A, Cerpa W, Tapia-Rojas C, Quintanilla RA. Genetic ablation of tau improves mitochondrial function and cognitive abilities in the hippocampus. Redox Biol. 2018;18:279–94. doi:10.1016/j.redox.2018.07.010.
72. David DC, Hauptmann S, Scherping I, Schuessel K, Keil U, Rizzu P, et al. Proteomic and functional analyses reveal a mitochondrial dysfunction in P301L tau transgenic mice. J Biol Chem.

2005;280:23802–14. doi:10.1074/jbc.M500356200.

73. Quinlan CL, Orr AL, Perevoshchikova I V., Treberg JR, Ackrell BA, Brand MD. Mitochondrial complex II can generate reactive oxygen species at high rates in both the forward and reverse reactions. J Biol Chem. 2012;287:27255–64.
74. Moreno-Sánchez R, Hernández-Esquivel L, Rivero-Segura NA, Marín-Hernández A, Neuzil J, Ralph SJ, et al. Reactive oxygen species are generated by the respiratory complex II - evidence for lack of contribution of the reverse electron flow in complex I. FEBS J. 2013;280:n/a-n/a. doi:10.1111/febs.12086.
75. Anderson A, Bowman A, Boulton SJ, Manning P, Birch-Machin MA. A role for human mitochondrial complex II in the production of reactive oxygen species in human skin. Redox Biol. 2014;2:1016–22.
76. Müller M, Cheung KH, Foskett JK. Enhanced ROS generation mediated by alzheimer's disease presenilin regulation of InsP3R Ca2+ signaling. Antioxidants Redox Signal. 2011;14:1225–35. doi:10.1089/ars.2010.3421.
77. Ghosh D, LeVault KR, Barnett AJ, Brewer GJ. A reversible early oxidized redox state that precedes macromolecular ROS damage in aging nontransgenic and 3xTg-AD mouse neurons. J Neurosci. 2012;32:5821–32. doi:10.1523/JNEUROSCI.6192-11.2012.
78. Su B, Wang X, gon Lee H, Tabaton M, Perry G, Smith MA, et al. Chronic oxidative stress causes increased tau phosphorylation in M17 neuroblastoma cells. Neurosci Lett. 2010;468:267–71.
79. Barbagallo M, Marotta F, Dominguez LJ. Oxidative stress in patients with Alzheimer's disease: Effect of extracts of fermented papaya powder. Mediators of Inflammation. 2015;2015.
80. Hensley K, Maidt ML, Yu Z, Sang H, Markesbery WR, Floyd RA. Electrochemical analysis of protein nitrotyrosine and dityrosine in the Alzheimer brain indicates region-specific accumulation. J Neurosci. 1998;18:8126–32. doi:10.1523/jneurosci.18-20-08126.1998.
81. Takesue T, Kawakubo H, Hayashida T, Tsutsui M, Miyao K, Fukuda K, et al. Downregulation of cytochrome c oxidase 1 induced radioresistance in esophageal squamous cell carcinoma. Oncol Lett. 2017;14:4220–4. doi:10.3892/ol.2017.6699.
82. Bourges I, Ramus C, Mousson De Camaret B, Beugnot R, Remacle C, Cardol P, et al. Structural organization of mitochondrial human complex I: Role of the ND4 and ND5 mitochondria-encoded subunits and interaction with prohibitin. Biochem J. 2004;383:491–9. doi:10.1042/BJ20040256.
83. Thomas RR, Keeney PM, Bennett JP. Impaired complex-I mitochondrial biogenesis in parkinson disease frontal cortex. J Parkinsons Dis. 2012;2:67–76. doi:10.3233/JPD-2012-11074.
84. Fløynes IH, Fernandez-Vizarra E, Lykouri M, Brakedal B, Skeie GO, Miletic H, et al. Neuronal complex I deficiency occurs throughout the Parkinson's disease brain, but is not associated with neurodegeneration or mitochondrial DNA damage. Acta Neuropathol. 2018;135:409–25. doi:10.1007/s00401-017-1794-7.
85. Adav SS, Park JE, Sze SK. Quantitative profiling brain proteomes revealed mitochondrial dysfunction in Alzheimer's disease. Mol Brain. 2019;12:8. doi:10.1186/s13041-019-0430-y.

86. Mendonça CF, Kuras M, Nogueira FCS, Plá I, Hortobágyi T, Csiba L, et al. Proteomic signatures of brain regions affected by tau pathology in early and late stages of Alzheimer's disease. Neurobiol Dis. 2019;130:104509.
87. Chen G, Ward BD, Chen G, Li SJ. Decreased effective connectivity from cortices to the right parahippocampal gyrus in Alzheimer's disease subjects. Brain Connect. 2014;4:702–8. doi:10.1089/brain.2014.0295.
88. Criscuolo C, Fontebasso V, Middei S, Stazi M, Ammassari-Teule M, Yan SS, et al. Entorhinal Cortex dysfunction can be rescued by inhibition of microglial RAGE in an Alzheimer's disease mouse model. Sci Rep. 2017;7:1–15. doi:10.1038/srep42370.
89. Diner I, Nguyen T, Seyfried NT. Enrichment of detergent-insoluble protein aggregates from human postmortem brain. J Vis Exp. 2017;2017.
90. Fein JA, Sokolow S, Miller CA, Vinters H V., Yang F, Cole GM, et al. Co-localization of amyloid beta and tau pathology in Alzheimer's disease synaptosomes. Am J Pathol. 2008;172:1683–92. doi:10.2353/ajpath.2008.070829.
91. Tai HC, Serrano-Pozo A, Hashimoto T, Frosch MP, Spires-Jones TL, Hyman BT. The synaptic accumulation of hyperphosphorylated tau oligomers in alzheimer disease is associated with dysfunction of the ubiquitin-proteasome system. Am J Pathol. 2012;181:1426–35. doi:10.1016/j.ajpath.2012.06.033.
92. Cummins N, Tweedie A, Zuryn S, Bertran-Gonzalez J, Götz J. Disease-associated tau impairs mitophagy by inhibiting Parkin translocation to mitochondria. EMBO J. 2019;38. doi:10.15252/embj.201899360.
93. Cook C, Kang SS, Carlomagno Y, Lin WL, Yue M, Kurti A, et al. Tau deposition drives neuropathological, inflammatory and behavioral abnormalities independently of neuronal loss in a novel mouse model. Hum Mol Genet. 2015;24:6198–212. doi:10.1093/hmg/ddv336.
94. Sahara N, Murayama M, Higuchi M, Suhara T, Takashima A. Biochemical distribution of tau protein in synaptosomal fraction of transgenic mice expressing human p301l tau. Front Neurol. 2014;5 MAR. doi:10.3389/fneur.2014.00026.
95. Zhou L, McInnes J, Wierda K, Holt M, Herrmann AG, Jackson RJ, et al. Tau association with synaptic vesicles causes presynaptic dysfunction. Nat Commun. 2017;8:1–13. doi:10.1038/ncomms15295.

Figures

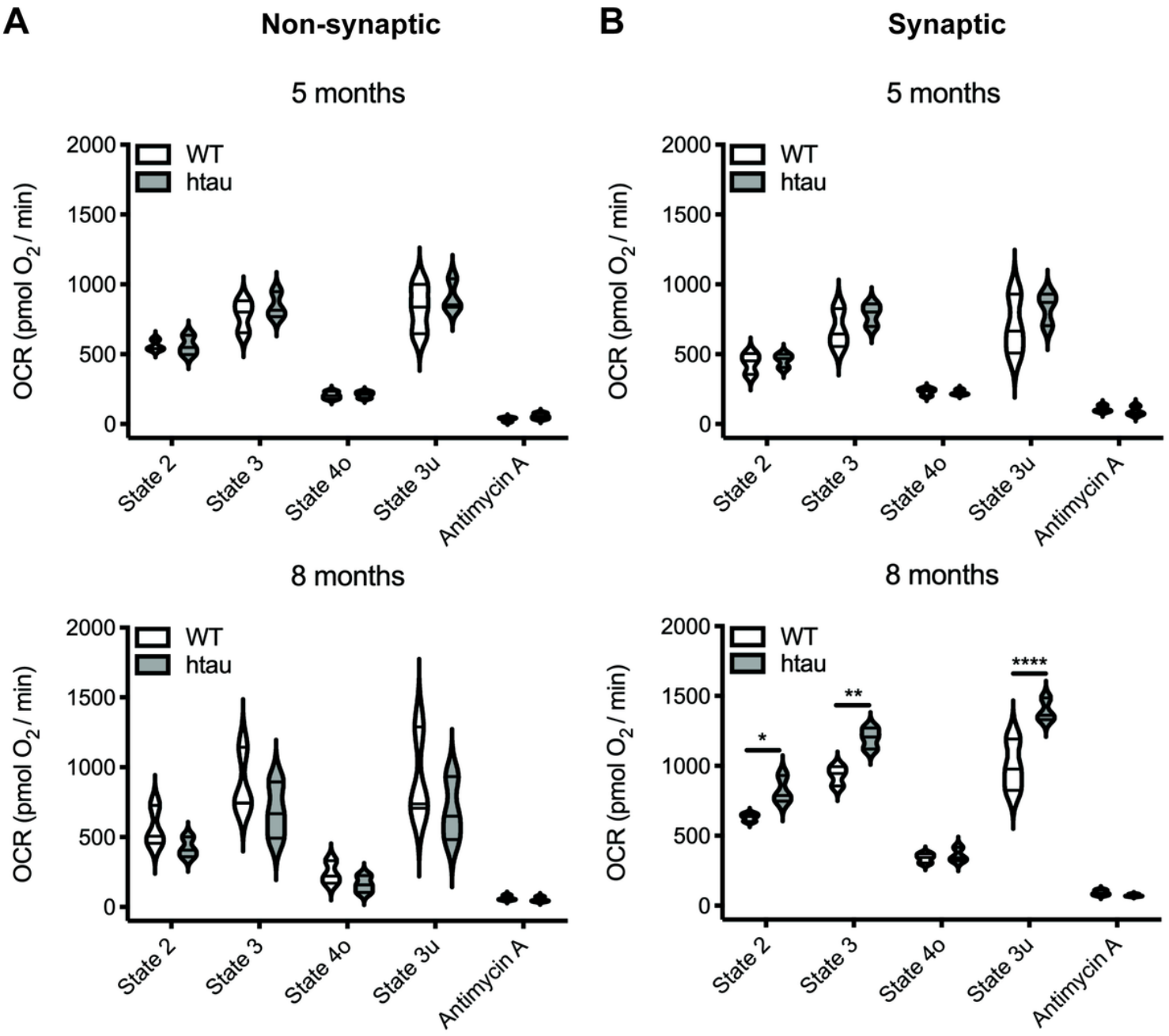

Figure 1

Tau expression alters synaptic mitochondrial respiration. Synaptic and non-synaptic mitochondria were isolated by discontinuous Percoll density gradient centrifugation from 5- and 8-month-old WT and htau mice and complex II-driven mitochondrial respiration (A-D) was assessed using a SeaHorse XFe24 Analyzer with the coupling assay. SeaHorse quantifications were normalized to protein content on a per well basis. Statistical significance was determined by 2-way ANOVA with Sidak's multiple comparisons test (* $p<0.05$, ** $p<0.001$, **** $p<0.0001$; $n = 3$, with 3 or 4 technical replicate wells)

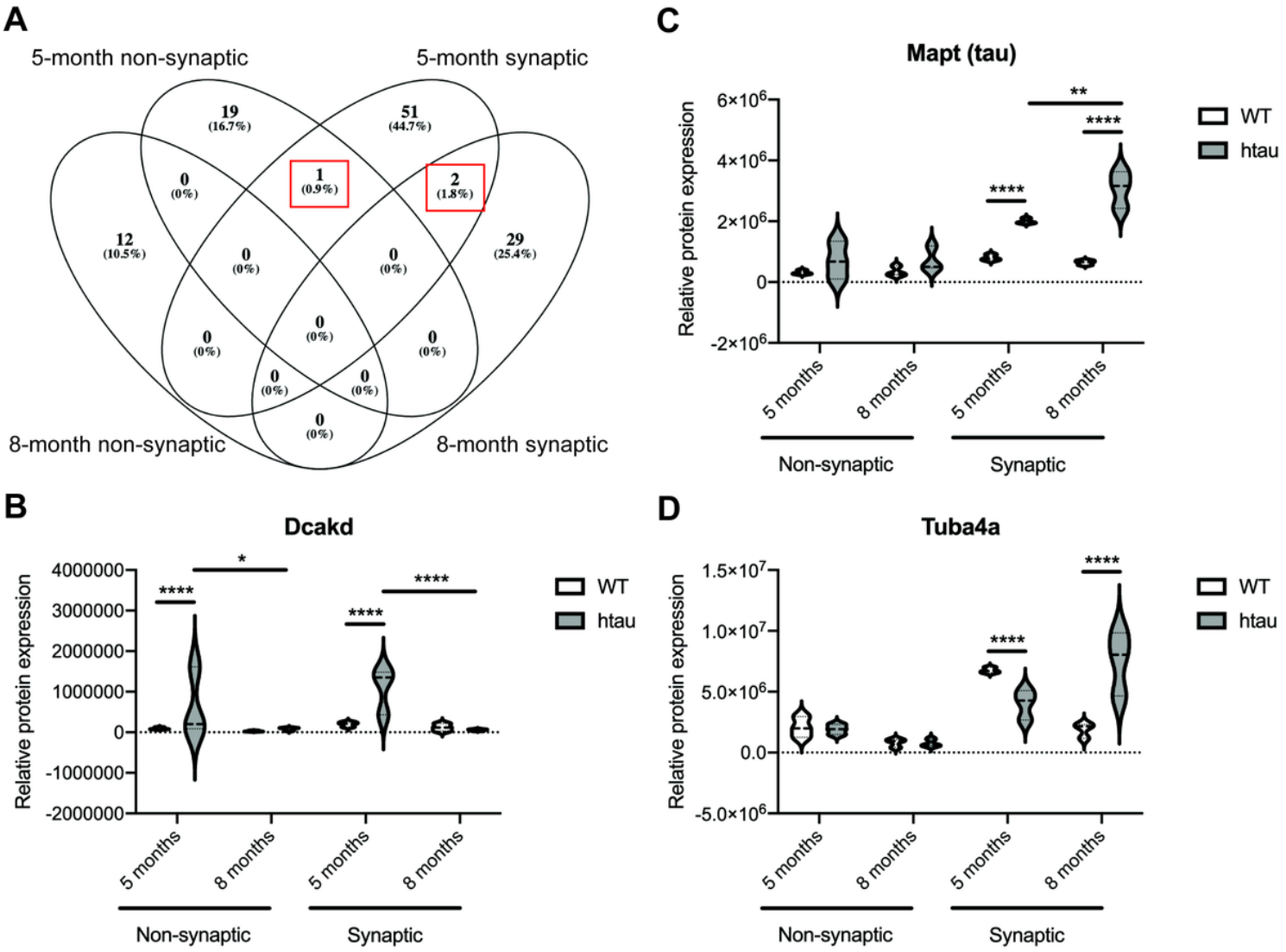

Figure 2

SWATH analysis reveals age- and tau-dependent alterations in the mitochondrial proteome. Isolated synaptic and non-synaptic mitochondria from 5- and 8-month-old WT and hTau mice were subjected to SWATH based proteomic analysis and Western blot. A) Venn diagram summarizing differentially expressed proteins between WT and htau synaptic and non-synaptic mitochondria at 5- and 8-months of age. B-D) Quantification of expression of Dcakd (B), Mapt (tau; C), and Tuba4a (D) determined by SWATH analysis. Statistical significance for SWATH results were determined by Cyber-T using Bayesian regularized t-tests with TukeyHSD pairwise post-hoc tests and Benjamini & Hochberg multiple test corrections (* $p<0.05$, ** $p<0.01$, ****$p<0.0001$; n = 3).

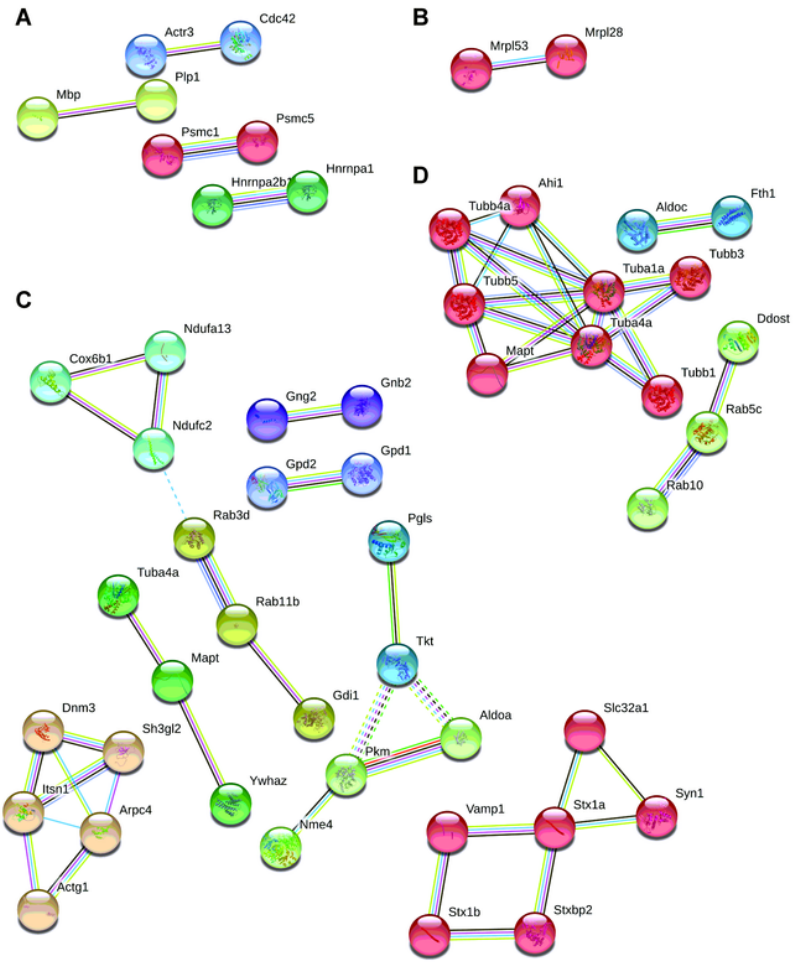

Figure 3

STRING analysis identifies key protein-protein interaction networks. STRING analysis was performed on the differentially expressed proteins for A) 5-month non-synaptic, B) 8-month non-synaptic, C) 5-month synaptic, D) 8-month synaptic. Clustering was performed using the MCL method, with a required minimum interaction score of 0.7 or greater (high confidence). Node (represent proteins) color corresponds to a cluster. Network edge (represent protein-protein interactions) color indicates the type of interaction evidence (teal: from curated database, magenta: experimentally derived, green: gene neighborhood, red: gene fusions, blue: gene co-occurrence, light green: textmining, black: co-expression, purple: protein homology)

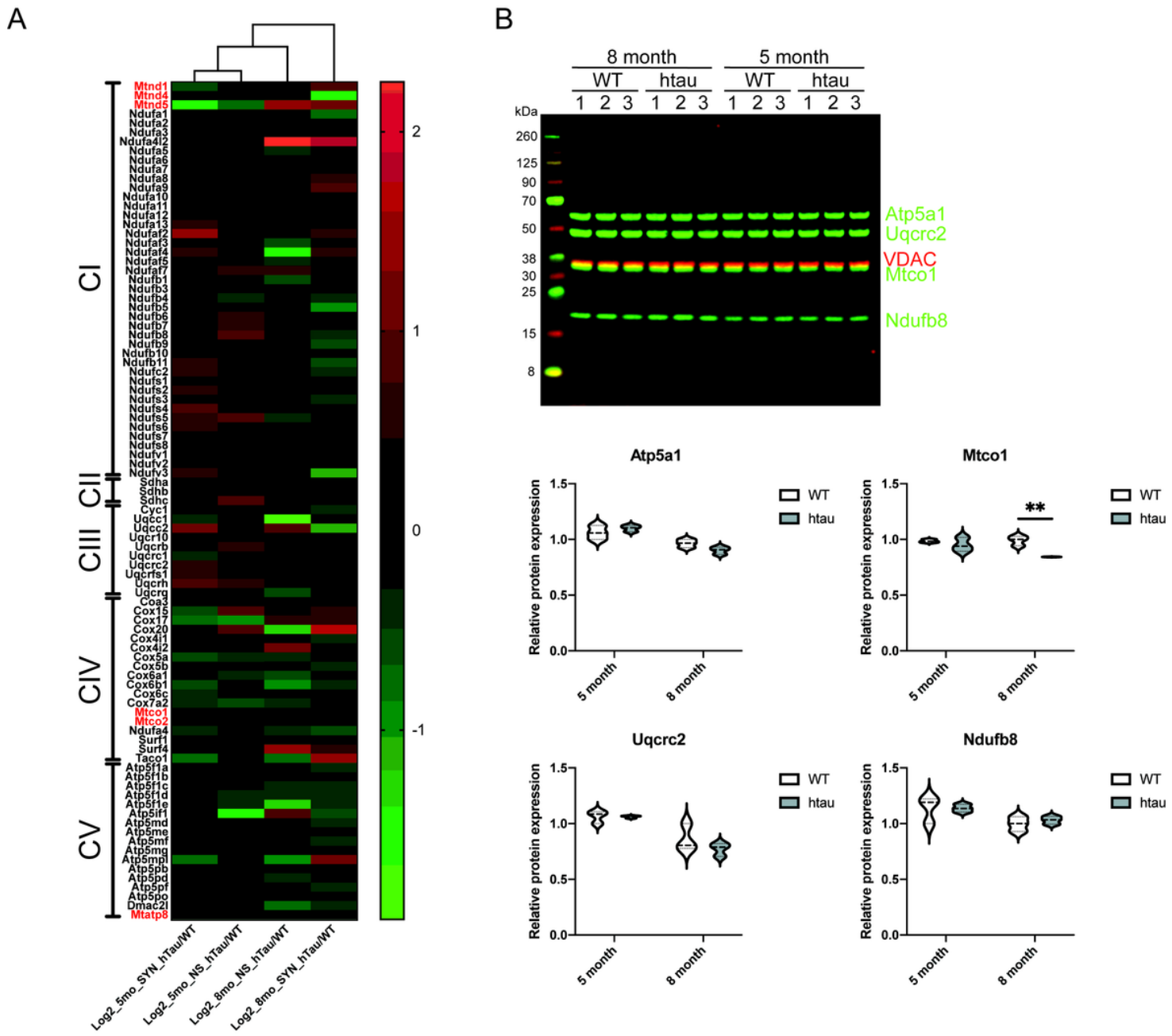

Figure 4

Expression of electron transport chain components is altered in aged htau mice. A) Log2-fold changes in expression of ETC components in synaptic and non-synaptic mitochondria determined by SWATH-MS were clustered using the Multiple Experiment Viewer web server to compare changes in expression between genotypes. Mitochondrial encoded subunits of the ETC that were detected and quantifiable are highlighted in red. The respiratory complex each group of proteins in the heatmap belongs to, is indicated with brackets (CI – complex I; CII – complex II; CIII – complex III; CIV – complex IV; CV – complex V). B) Synaptic mitochondria were isolated by discontinuous Percoll gradient from 5- and 8-month-old WT or htau mice, solubilized with SDS buffer and analyzed by immunoblot using the rodent OxPhos antibody cocktail (green) and VDAC (red). Quantification of immunoblots was done by densitometry, normalizing

the indicated OxPhos protein to the mitochondrial marker VDAC. Statistical significance was determined by unpaired multiple T-Tests using the two-stage setup method (Benjamini, Krieger, and Yekutieli) (** p<0.01, n = 3).

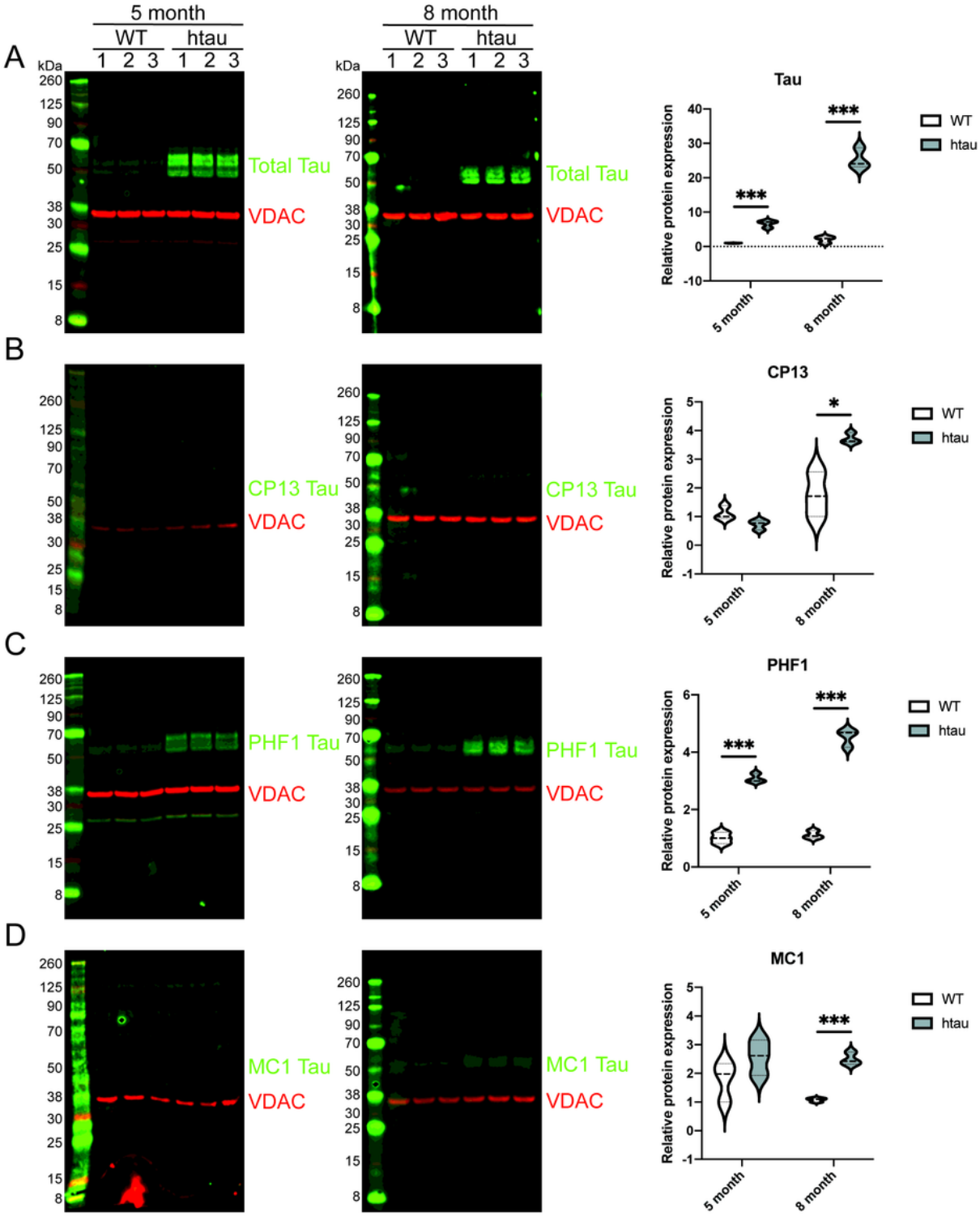

Figure 5

Total and pathogenic tau is elevated in synaptic mitochondrial isolates from of 8-month-old htau mice. Synaptic mitochondria were isolated by discontinuous Percoll gradient from 5- and 8-month-old WT or

htau mice, solubilized with SDS buffer and analyzed by immunoblot for A) total and B-D) pathological forms of tau (green). Quantification of immunoblots was done by densitometry, normalizing the indicated tau form to the mitochondrial marker VDAC (red). Statistical significance was determined by multiple T-Tests using the two-stage setup method (Benjamini, Krieger, and Yekutieli) (* p<0.05, *** p<0.001, n = 3).

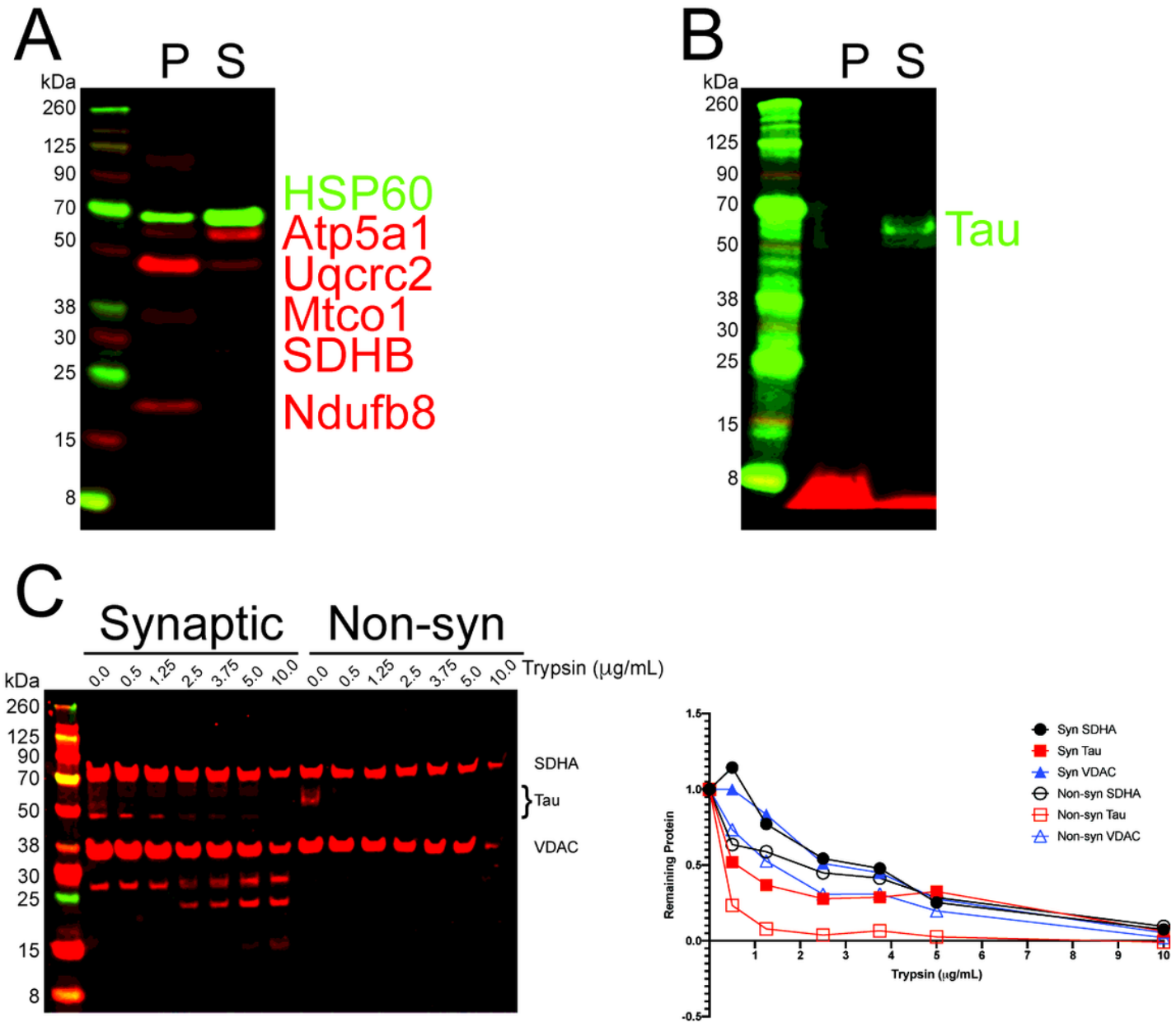

Figure 6

Mitochondrial associated tau is not membrane integrated. A-B) Mitochondria isolated from 8-month-old htau mice were incubated on ice in a sodium carbonate extraction buffer and fractionated by ultracentrifugation to differentiate membrane associated from membrane-integrated proteins. The resulting fractions were assessed by immunoblot for the indicated proteins (P = pellet/insoluble (membrane-integrated), S = soluble (membrane associated) A) Blot for HSP60 and OxPhos as representative controls for the assay. B) Blot of total tau. C) Synaptic and non-synaptic mitochondria isolated from 8-month-old htau mice were digested with the indicated concentration of Trypsin on ice for

30 min, and then solubilized with SDS buffer and analzyed by immunoblot for total tau, SDHA, and VDAC to determine the exent of protease digestion.

Supplementary Files

This is a list of supplementary files associated with this preprint. Click to download.

- AdditionalFile1.xlsx
- FigureS1.tif
- FigureS2.tif
- FigureS3.tif
- FigureS4.tif